Received: 5 October 2022 | Revised: 4 December 2022 | Accepted: 5 December 2022

DOI: 10.1002/rcm.9454

RESEARCH ARTICLE

Rapid Communications in Mass Spectrometry WILEY

Depth profiling and standardization from the back side of a sample for accurate analyses: Emphasis on quantifying low-fluence, shallow implants in diamond-like carbon

Karen D. Rieck[1,2,3] | Amy J. G. Jurewicz[4,5] | Richard L. Hervig[2] | Peter Williams[6] | Chad T. Olinger[7] | Roger C. Wiens[3,8] | Ryan C. Ogliore[9]

[1]New Mexico Consortium, Los Alamos, NM, USA

[2]School of Earth and Space Exploration, Arizona State University, Tempe, AZ, USA

[3]Space Remote Sensing and Data Science, Los Alamos National Laboratory, Los Alamos, NM, USA

[4]Buseck Center for Meteorite Studies, School of Earth and Space Exploration, Arizona State University, Tempe, AZ, USA

[5]Department of Earth Sciences, Dartmouth College, Hanover, NH, USA

[6]School of Molecular Sciences, Arizona State University, Tempe, AZ, USA

[7]US Department of Energy Germantown, Germantown, MD, USA

[8]Earth, Atmospheric, and Planetary Sciences, Purdue University, West Lafayette, IN, USA

[9]Department of Physics, Washington University in St Louis, St Louis, MO, USA

Correspondence
K. D. Rieck, New Mexico Consortium, 4200 West Jemez Road, Suite 200, Los Alamos, NM 87544, USA.
Email: krieck@newmexicoconsortium.org

Funding information
NSF Division of Earth Sciences, Grant/Award Number: EAR0622775, NASA, Grant/Award Numbers: 80NSSC19K1239, 80NSSC22K0589, NNH09ZDA001N, NNH15AZ67I, NNX09AC35G, PLANET14R0012. US DOE Grant/Award Number: DEAC0206CH11357

Rationale: Back-side thinning of wafers is used to eliminate issues with transient sputtering when analyzing near-surface element distributions. Precise and accurate calibrated implants are created by including a standard reference material during the implantation. Combining these methods allows accurate analysis of low-fluence, shallow features even if matrix effects are a concern.

Methods: Implanted Na (<2.0×10^{11} ions/cm^2, peaking <50 nm) in diamond-like carbon (DLC) film on silicon (solar wind returned by NASA's Genesis mission) was prepared for measurement as follows. Implanted surfaces of samples were epoxied to wafers and back-side-thinned using physical or chemical methods. Thinned samples were then implanted with reference ions for accurate quantification of the solar wind implant. Analyses used a CAMECA IMS 7f-GEO SIMS in depth-profiling mode.

Results: Back-side-implanted reference ions reduced the need to change sample mounts or stage position and could be spatially separated from the solar wind implant even when measuring monoisotopic ions. Matrix effects in DLC were mitigated and the need to find an identical piece of DLC for a reference implant was eliminated. Accuracy was only limited by the back-side technique itself.

Conclusions: Combining back-side depth profiling with back-side-implanted internal standards aides quantification of shallow mono- and polyisotopic implants. This technique helps mitigate matrix effects and keeps measurement conditions consistent. Depth profile acquisition times are longer, but if sample matrices are homogeneous, procedural changes can decrease measurement times.

1 | INTRODUCTION

1.1 | Overview

Accurate and calibrated analysis of low-concentration implants situated very near the surface of a substrate is highly challenging. The technique reported here allows quantification whether or not a suitable matrix-appropriate standard is available from vendors and allowed us to accurately and precisely quantify low concentrations of elements located within 500 nm of a wafer's surface. Moreover, application to analyses of trace, near-surface elements in anhydrous, amorphous tetrahedrally coordinated diamond-like carbon (DLC or ta-C) demonstrates that internal standardization, the basis of this technique, can mitigate matrix effects in some nonuniform samples.[1,2]

The driving force for developing this technique was issues encountered measuring solar wind (SW) collected and returned to Earth by NASA's Genesis[3,4] spacecraft. The entire SW sample was the mass equivalent of a few grains of salt but spread out over several square meters of collection surface. Moreover, the task of the analysts was to analyze minor elements in this SW sample. The element used herein, Na, was estimated to be present at less than 2×10^{11} SW Na^{+}/cm^{2} with a peak implantation depth of only *ca* 25 nm in DLC on silicon (Figure 1) collectors. Na was selected for this study to demonstrate the benefits of back-side depth profiling (BDP) with back-side internal standardization, because although it is possible to measure this element in Genesis collectors with front-side depth profiling, it is very difficult to do so. This difficulty is compounded by a further complication that – upon return to Earth – the solar wind collectors were shattered and their surfaces were exposed to terrestrial contaminants and spacecraft debris due to an unplanned, spectacular hard landing.[4–6] Many of the contaminants and debris could not be removed without risking damage to the precious, near-surface SW sample.[1,6–8] Flight silicon collectors were easily etched at the nanometer scale by standard semiconductor cleaning techniques and this etching was clearly affected by the radiation damage caused by the SW implantation itself.[7,9] The radiation damage and related changes to some samples were primarily due to the high doses of the two most abundant SW elements (hydrogen: 1.634 (± 0.028; 2 sigma SD) $\times 10^{16}$ H/cm^{2}; and helium: *ca* 8.5 (± 0.7; standard deviation of the mean) $\times 10^{14}$ He/cm^{2})[10,11] as other elements in the periodic table were present in doses orders of magnitude lower.

DLC is a robust material – more easily cleaned and not prone to radiation-enhanced segregation.[8] Because the SW ions did not diffuse significantly in the amorphous DLC after implantation, ion implant modeling codes such as SRIM provide accurate results. However, in DLC, the SW H can change the ion yield of the matrix ions (e.g. C–H formation lowers C counts)[12] during analysis by secondary ion mass spectrometry (SIMS).

The hydrogen implant also changes the composition of the secondary ions during SIMS analysis, and this composition varies depending on the electrical conductivity and structural properties (including texture) of the DLC. Genesis DLC is an inhomogeneous material – a combination of graphite and diamond. In previous work on Mg isotopes in DLC,[8,12] we looked at the yield of ($^{24}MgH + {}^{25}Mg$)/^{24}Mg versus the yield of $^{26}Mg/^{24}Mg$. From our data we were able to infer that ^{24}MgH was not correlated with ^{25}Mg. Rather, its abundance appeared to be a function of the heterogeneous matrix.

Depending upon instrument set-up and the local matrix it is probable that, as we found for ^{24}Mg, some combinations of conditions would cause significant hydration of the implanted ions (here, Na) as well, reducing the intensity of the atomic signal we are measuring. So, even if DLC standards were commercially available, it would have required additional testing (perhaps with Raman) to see what portions of that standard, if any, corresponded to the matrix of the Genesis sample.

In short, making accurate SW implant measurements required not only low detection limits, but also that all terrestrial contaminants were excluded, and that matrix effects in the DLC were mitigated. Moreover, although standards are often available for silicon, standardization of DLC would always be complicated by inhomogeneity. Therefore, the study reported here applied several methods, both conventional and recently developed methods as described below.

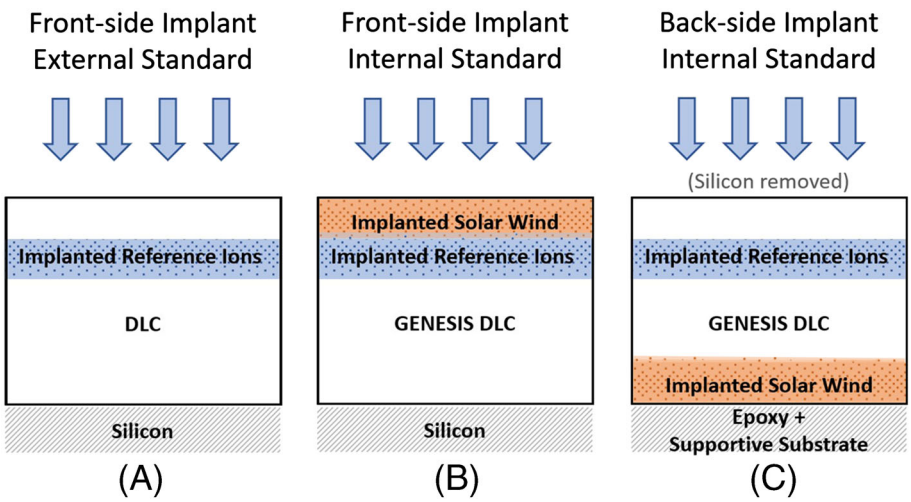

FIGURE 1 Schematic edge-on view illustrating three types of reference implants created for this study: (A) typical reference; (B) internal front-side reference as per Huss et al.[12]; (C) internal back-side reference (new, this work and Rieck[1]). The thickness of the DLC is 1 μm. Each sample is *ca* 5 mm wide. Implant depths are approximated. Note: (C) shows SW (our unknown near-surface layer), but that layer could also be a previous standard implant to be used for intercalibration. The supportive substrates used for (C) were GaAs wafer or carbon planchets. [Color figure can be viewed at wileyonlinelibrary.com]

1.2 | Background: methods combined to produce our novel technique

The general methods used in combination for this study were BDP, calibration using ion implants into a standard reference material ("internal standardization"),[13] and the use of "templates"[10] or, in DLC only, SRIM models to correct artifacts in SIMS depth profiles.[12] Each of these methods detailed below has been used elsewhere (separately) for both Genesis and other samples.

BDP is commonly used for measuring the composition and/or diffusion of near-surface layers in semiconductor devices and was first routinely applied to Genesis silicon collectors by Heber et al.[15] This method entails that the surface of the sample first be epoxied to a conductive (usually silicon) substrate. Then the back of that sample is ground to a preferred thickness – one that is thin enough that: (1) the time needed to sputter through the sample is relatively short and (2) there is no topography in the sputtered crater caused by the ion beam, but (3) the sample is thick enough that transient sputtering effects (and any ion-mixed contamination) are isolated from the thin layer containing the unknown elements of interest. This "ideal" thickness is usually between 0.5 and 1 μm. However, for Genesis DLC-on-silicon wafers all the silicon was removed and the DLC layer remained as fabricated,[1] *ca* 1 μm thick. Because the DLC film is highly stressed and fragile, removing the silicon backing by grinding is usually ineffective: the film can buckle or shatter when grinding near the DLC–silicon interface.[1] However, XeF_2 etching will remove the silicon backing from the thin DLC films to enable BDP.[1,16]

"Internal standardization" covers several related techniques which rely upon the simultaneous implantation of ions of the element of interest into several materials, one of which is a standard reference material or a secondary standard. Using the difference in counts between the *implanted* reference material versus the *unimplanted* reference material, the implant can be calibrated. Then, that calibrated implant can be used as a secondary standard. If that same implant was implanted into the sample to be analyzed and the reference material simultaneously, then the implant is referred to as an *internal standard*. Although not commonly used at the moment, internal standardization (one technique used for analyzing Genesis samples) has many possible applications[14,17,18] as it helps to mitigate matrix effects, differences in height or tilt between the sample and standard that may cause variation in ion yields, and inadvertent changes to instrumental conditions between measurement of sample and standard.

Prior to this work, internal standards were minor ions implanted at similar or deeper depths than the major ion implant to be quantified; if the element to be quantified had only one isotope, the reference ions were implanted at an energy such that the peak was significantly deeper than the layer of interest. In contrast, for this work the reference implant is implanted into the back side so that the chance of the reference implant contaminating the ions to be measured is minimized. In addition, possible issues with instrumental mass fractionation can be avoided because the reference implant can always be the same isotope as the one being analyzed. Indeed, this work was motivated by the fact that Na is monoisotopic, so distinguishing a ^{23}Na reference implant from the SW ^{23}Na implant was challenging unless the implants were well separated spatially.

While the combination of BDP and internal standardization enhances accuracy, there is still the issue encountered in *all* BDP work measuring ultra-shallow implants: knowing exactly where the data have been collected relative to the original surface of the sample (see Rieck[1] and references therein). Minor tilting of the sample can cause an uneven breakthrough, obscuring the depth of the original surface. Worse, when an element is mobile (such as Na), an uneven breakthrough is a chance for that element to move from the edge of the crater along the crater surface to contaminate the analyzed area.

One method currently under development for mitigating the issues with BDP mentioned above is based on ion imaging.[18] Specifically, ion images taken during the breakthrough of the sputtered crater into the substrate underlying the sample are deconvolved, or flattened, through image analysis techniques to create a depth profile that reaches the surface uniformly. However, to simplify this current test of back-side implantation, we decided to skip the ion imaging step, because it is still under development. However, we do expect that this technique will be used with the technique described herein to further reduce errors in quantification. We tested the use of templates to match the shape of each depth profile to a reference depth profile, a method adapted from Huss et al.[10] But for DLC, SRIM was easy to use and successful in extrapolating the data to the interface,[12] although the quantification is dependent upon accurate knowledge of the sputtering rate. We have found that a useful anchor for both the template and SRIM methods of extrapolating the unknown implant to the surface is the use of a pre-existing, well-characterized front-side implant. In the work reported here, we used the well-characterized SW ^{24}Mg implant[8,12] to precisely locate the collection surface of the DLC.

2 | EXPERIMENTAL

2.1 | General sample preparation

A general overview of sample preparation methods is provided here, and full details are provided by Rieck.[1] First, the DLC-on-silicon collectors were cleaned with a series of solvents using modified RCA cleaning methods[1,19] to remove as much of the crash debris as possible. Then, the samples were mounted face down on rigid, conductive substrates for thinning. These substrates also needed to be resistant to XeF_2 so we used either GaAs or a carbon planchet.

In the semiconductor industry, thinning methods are usually used for silicon, and the wafers are simply mechanically back-side-polished. However, the intrinsic stresses in the Genesis DLC on silicon make the DLC film fragile, and since DLC is relatively inert, chemical etching is less likely to damage the film. Accordingly, we used XeF_2 etching to remove the silicon supporting the DLC. Note that the DLC film itself was not thinned; the back-side reference implant was chosen to fit into the *ca* 1 μm thick layer without overlap of the SW. The etching was done in a Xactix® X4 Series™ XeF_2 etch system at Argonne

National Laboratory using procedures developed by Veryovkin et al.[16] When the silicon had been removed and the back-side of the DLC fully exposed, the samples were removed from the chamber and compressed air was used to remove any residue from the etch (more details in Rieck[1]).

2.2 | Reference implantation

For ion implantation, samples were mounted on stainless steel plates (with multiple samples per plate) using conductive materials to ensure grounding, according to the methods of Burnett et al.[14] Two separate batches of implants were performed. Figure 1 illustrates the samples included in the implantations. Each plate was uniformly implanted with ^{23}Na by Leonard Kroko, Inc. (Tustin, California). SRIM models combined with the results of earlier analyses of standard implants were used to select a suitable reference ion energy (100 keV). The nominal 2.0×10^{12} $^{23}Na^{+}/cm^{2}$ dose was later checked by SIMS analysis, using high-dose standards calibrated using Rutherford backscattering spectrometry.[1] The results verified that the two batches had nearly identical doses: 1.94×10^{12} and 1.95×10^{12} $^{23}Na^{+}/cm^{2}$.

Blank silicon was included in each batch for implant intercalibration with existing standards. One back-side-thinned calibrated implant into silicon was also included on one plate for ease of calibration; unfortunately, the sample was accidentally over-thinned by the vendor. The result was that the new reference ^{23}Na implant was not fully separated from the ^{23}Na calibrated implant, rendering that particular sample unusable.

2.3 | Preparation after implantation

After removal from the plates, the backs of every sample were wiped with acetone to remove residual adhesive. A second solvent cleaning was used on wafer fragments, but solvent cleaning on thinned samples had inconsistent (and generally disastrous) results.[1] Therefore, back-side-thinned samples were not re-cleaned after implantation and the exposed (back side) surface was "as implanted" for SIMS analysis. The surfaces of the thinned samples were photographed in great detail, with an emphasis on the (weak) thin-film interference patterns visible after thinning. The high stress state of the DLC films occasionally created crossing, contradictory interference fringes and topography, and occasionally showed features due to crash-induced damage or particulates or interference patterns from underlying epoxy.[1] The photographs were intended for (1) avoiding features that indicated defects and for (2) finding areas with interference patterns that suggested a uniform sample thickness.

2.4 | Analytical conditions

Reference implant calibrations were performed in the NSF-funded Secondary Ion Mass Spectrometry Lab at ASU on its CAMECA IMS 6f. These were all front-side analyses of front-side implants into silicon co-implanted alongside the thinned DLC samples as in Burnett et al.[13] Analyses of internally standardized samples were conducted using the CAMECA IMS 7f-GEO SIMS at the Caltech Microanalysis Center. Details for the reference ion calibrations are given in Rieck.[1] An overview of the SW analyses is given here. Details are given in the supporting information and Rieck.[1]

For the SW analyses, because the SIMS technique was being tested and in the process of optimization, various instrument conditions were used. All analyses used an O_2^+ primary ion beam at a low (6 keV) impact energy (13 kV source voltage, 7 kV sample voltage). The combination of O_2^+ and a low impact energy was chosen for increased depth resolution. Custom-made inserts positioned samples in the exact center of the holder to mitigate any issues with electromagnetic field variations due to location on the mount. Raster sizes were 100×100 μm^2 and 120×120 μm^2. Beam currents were approximately 20 to 40 nA. Resulting sputtering rates were *ca* 1–3 Å/s. Conditions were chosen to keep implant peak count rates at *ca* 1×10^5 counts/s on the standard implant to mitigate the effect of instrumental deadtime on measurements. To mask ions scattered from the walls of the crater, we used a 400 μm field aperture, which excludes most secondary ions from outside a 35 (±5) μm diameter area of the crater floor. To further reduce signal from walls, we also used electronic gating (30–80%). Mass resolving power was $1200M/\Delta M$, except for a front-side depth profile, which used a mass resolving power of 2500, so that we could also measure a second reference implant ($^{41}K^{+}$), without risking interference from a potential matrix species ($^{28}Si^{13}C^{+}$). Other parameters were also varied as we adjusted the technique in attempts to optimize conditions for the target element, Na. Details of parameters for all analyses are given in the table "Analytical Parameters" in Rieck[1] and in Section I.A (supporting information).

2.5 | Data collection technique

The back-side depth profiles for the SW were performed in steps similar to those of Heber et al.[15] That is, for back-side depth profiles, the initial step was to collect the unknown ion (Na^{+}) and a matrix ion ($^{12}C^{+}$). After profiling through the reference implant to the background Na intensity, background data were collected for tens of minutes. Then the analysis was stopped and the matrix ions were removed from the analysis routine to optimize sampling rate at the sample surface. This did not pose a problem for Na normalization, because the C count rate does not track with Na near the collector surface. The $^{12}C^{+}$ count rate changes through the SW H implant – likely caused by a matrix effect (see Section III.C.iii, including Figure III.C.4, supporting information) – rendering the matrix ion intensity in this region unusable for normalizing the Na signal. Instead, we extrapolated the matrix ion count rate from the first portion of the profile through the SW portion to normalize the Na count rate. No other conditions were changed (e.g. raster size and beam current were kept the same; see Section 1.A, supporting information). The

analysis was then restarted with the unknown (but no matrix ions) and was run through the breakthrough of sample into the epoxy–substrate. Sometimes ^{24}Mg was also included in this step for *in situ* tracking of depth near the collection surface. A discussion of the data reduction is provided in the sections below and in Section I.B (supporting information). A discussion of the underlying assumptions of this approach is provided in Section II (supporting information).

The DLC film was only *ca* 1 μm thick, so significant roughening of the crater floor during sputtering was not expected. Even so, small amounts of roughness were observed. Grooves near the crater walls (e.g. Figure III.C.1, Section III.C.ii, supporting information) were probably due to issues with the software controlling the raster, but most secondary ions from these grooves would have been excluded through the use of the field aperture and electronic gating. Other roughness that caused uneven breakthrough at the DLC–epoxy interface may have been due to crash debris, crash-induced damage, or wrinkling of the DLC film after thinning. For back-side analyses, crater floor roughening increased the depth from the collector surface from which we could measure SW, but in spite of this issue, we were able to measure uncontaminated SW and recover the remaining portion using SRIM models.

If these DLC samples were as homogeneous as (flight spare) silicon wafers, we could have measured the internal implant separately from the SW without matrix effects. Although the DLC films have only minor textural variations with depth (e.g. crystallites, annealing layers), and their electrical properties are effectively homogeneous with depth[8,20] (see also Section III.A, supporting information), the electrical properties (and thus matrix effects) in DLC can vary greatly (horizontally) across a 500 μm × 500 μm crater.[8,12,20] Therefore, separating analyses of the reference and unknown laterally would have negated the boundary conditions (and, therefore, usefulness) of the internal implant.

2.6 | Data reduction

2.6.1 | Correcting the data

Prior to quantification, corrections must be made to the raw SIMS data to eliminate various artifacts. As noted above, background is always measured directly and can be easily subtracted. Corrections for primary beam drift were somewhat of an issue herein because our CAMECA IMS 7f-GEO depth profiling program did not measure current for each duty cycle. When available, the change in matrix counts was used as a proxy; when matrix counts were not available, the change in beam current was estimated to be linear between the measurement of starting and ending currents. We note that a small linear increase in beam current gives a small linear increase in matrix species, but the percentage change of beam current is not equal to that of matrix intensity. Therefore, to better estimate the yield of the matrix species, we calculated the slope describing the change in matrix species intensity with the change in current, using matrix species intensity and beam current (where available) for a different analysis conducted under similar conditions (Figure III.C.4, Section III.C.iii, supporting information). This estimate checked the total error of our calculations and was shown to reduce scatter (details in Section 3).

Transient sputtering and ion mixed surface contaminants affect the back-side-implanted reference implants as they are analyzed as standard front-side depth profiles. But these effects could be mitigated by implanting the reference ions such that the vast majority of the implant lies deeper than the zone of transient sputtering and ion mixed surface contaminants. Then, the small portion of the reference implant affected by these artifacts can be corrected using SRIM models or templates. The correction using SRIM models fits the calculated ion range to the unaffected portion of the reference ion depth profile, and the model is then used to extrapolate the intensity of the reference implant through the compromised zone near the surface.[13] In addition, a corrected back-side analysis of the reference implant could be used as a template (scaled to match the intensity of the peak and sputtering rate) to accurately correct other depth profiles.[12] In many cases, the magnitude of these corrections was within *ca* 6% of a straight-line extrapolation to the surface used as a preliminary estimate.[8]

In addition to the surface correction for the reference implant, the data needed to be corrected for issues inherent to all back-side depth profiles, regardless of whether an internal standard is present. That is, correcting the raw data for ion mixing (including "up-gardening" and "forward mixing") at the sample–epoxy interface and, since sputtered craters are almost always at a small angle to that interface, smearing of the depth profile intensities. In some instances, Na^+ can probably migrate into the analyzed area from areas of higher concentration (e.g. sample surface or epoxy) and enter the path of the secondary ions into the detector. Herein, we correct for these effects using templates and SRIM models. Again, because ions do not appear to move after implantation into DLC,[8,12] SRIM appears to give excellent extrapolations of the SW depth profiles near the sample–epoxy interface. Some depth profiles appeared stretched, probably due to ion mixing or, perhaps, "smearing" (e.g. from sample buckling). SRIM models can be artificially stretched by adding a silicon (Si) component to the target composition and/or by decreasing the density for calculation of the SRIM depth profile model. The effects of these techniques are presented in Sections 3 and 4 and the supporting information.

2.6.2 | Quantifying the data

The usual method of quantification of trace elements uses relative sensitivity factors (RSFs)[22] where, for an element Y:

$$RSF_Y = F_{std} / \int (I_Y / I_{matrix})_{std}\, dx \quad (1)$$

where F_{std} is the calibrated fluence of the reference implant for Y (in atoms/cm^2), I_Y is the secondary ion intensity measured for Y

(in counts per second), (I_Y/I_{matrix}) is the ratio of the Y intensity normalized to the intensity of a matrix species (I_{matrix}) for each duty cycle, and dx is the depth of the duty cycle. Then the fluence of the unknown is calculated as:

$$F_{unk} = RSF_Y \times \int (I_Y/I_{matrix})_{unk}\, dx = F_{std} / \int (I_Y/I_{matrix})_{std}\, dx \times \int (I_Y/I_{matrix})_{unk}\, dx \quad (2)$$

Note that internal standardization simplifies equation (2) if the matrix intensity (I_{matrix}) remains constant (i.e. no drifts in beam current or ion yield) throughout the analysis. That is, when $(I_{matrix})_{unk} = (I_{matrix})_{std}$, the calculation for the fluence of the unknown becomes:

$$F_{unk} = F_{std} \times \int (I_Y)_{unk}\, dx / \int (I_Y)_{std}\, dx \quad (3)$$

Of course, in the real world, current does drift and ion yields may change significantly in very deep craters. However, these are corrections to the intensity, and in theory the use of an RSF for an internal standard is not required in a homogeneous material if the instrument is stable. Note that DLC is sufficiently homogeneous in columns, but not laterally. Equation (3) is why internal standardization works extremely well on samples with matrix effects, whether it be DLC or sections containing multiple phases: the ratio of the intensities of the unknown to the implant is needed for quantification, but the matrix intensity does not directly factor into the quantification.

3 | RESULTS

Front-side internal standardization is a technique that has been proven to work for Genesis samples previously.[2,12] Accordingly, we first present the SW Na data and fluence from our successful front-side analysis in DLC (Figure 2) for use as a baseline. The advantage of front-side internal standardization and front-side analysis is that the sputtering rate can be easily determined by measuring crater depth directly and dividing by the analysis time, because the position of the collection surface is preserved. By definition, overlapping reference and SW implants have matrices with the same composition and density even when (as in this case) there are components such as H in the SW that are not implanted with the reference implant. The disadvantage of a front-side internal standardization and front-side analysis is that the internal standard had been implanted through the SW. Therefore, not only does the ion-mixed surface contamination need to be identified and removed, but quantification also requires deconvolving the signal of the internal implant from that of the SW. The deconvolution step is complicated by the fact that there was some broadening of the implants due to ion-beam mixing by the primary beam. The yellow arrow in Figure 2A shows where the broadening is most obvious.

For the front-side analysis presented in Figure 2, no single set of SRIM input parameters gave absolutely unequivocal fits to both the reference implant and the SW. Accordingly, several pairs of SRIM models were created for the reference implant and the unknown, each pair stretched using various convenient model parameters. These were then fitted to the data, each pair of SRIM models giving a different result. The range of the estimates was 7.42×10^{10} to

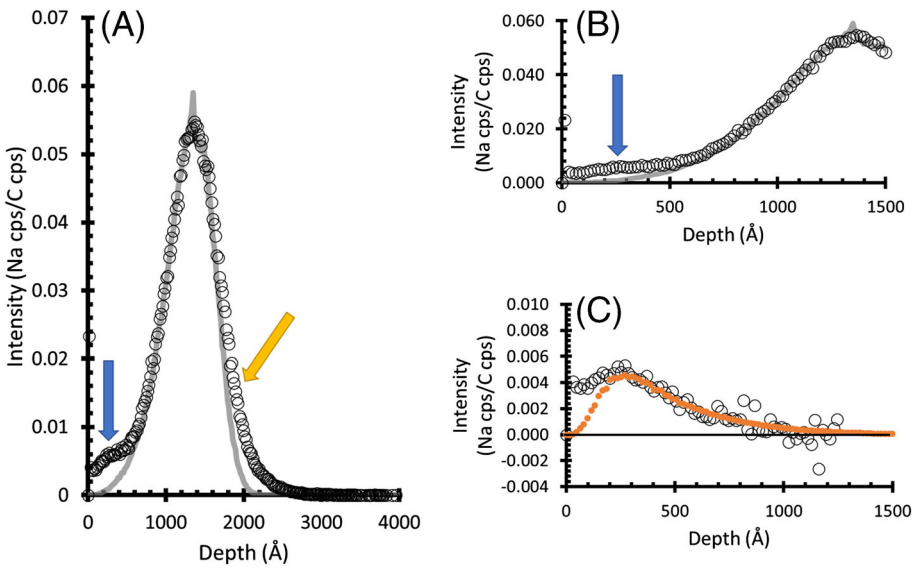

FIGURE 2 Front-side internally standardized SW Na measurement for use as baseline reference. Lines represent SRIM models. Yellow arrow points to profile broadening by ion mixing beyond what could be corrected using a low SRIM density. Blue arrows (A, B) point to "ion-mixed surface contaminants + SW," which are isolated in (C). The "ion-mixed surface contaminants" shown in (C) end at the peak of the SW SRIM model (orange dots), *ca* 250 Å. This rapid drop in surface Na could be real, but the back-side depth profiles generally show "dirt" mixed deeper. Accordingly, (C) indicates an upper limit for the calculated SW Na fluence for the assumptions of matrix density, composition, and sputtering rate (which were identical in the implant and SW SRIM models). [Color figure can be viewed at wileyonlinelibrary.com]

9.36×10^{10} Na^+/cm^2, with the mean fluence *ca* 8.37×10^{10} Na^+/cm^2. This range is plotted as the white bar in Figure 3, and additional information about these models is available in Section III.B (supporting information).

Figure 3 also shows the results from three back-side depth profiles. The inputs for the matrices of the internal back-side implant and the front-side SW implant were kept the same as for paired SRIM models. The error on sputtering rate was slightly larger, so sputtering rate was varied along with SRIM matrix parameters to achieve best fits to the data. The ranges of fluences for each analysis determined by stretching SRIM fits by changing matrix parameters and sputtering rates are given by the vertical bars in Figure 3. The horizontal gray box in Figure 3 estimates overlap between the best fits for the four analyses (*ca* 8.1 (±1.1) $\times 10^{10}$), where the width is the standard error of the mean. We note that this box width is meant to illustrate the consistency between front-side and back-side standardization, not to constrain Na fluences. Future work is required before accurate, precise Na fluences are reported, e.g. requiring H to be present in the standard and not just the SW.

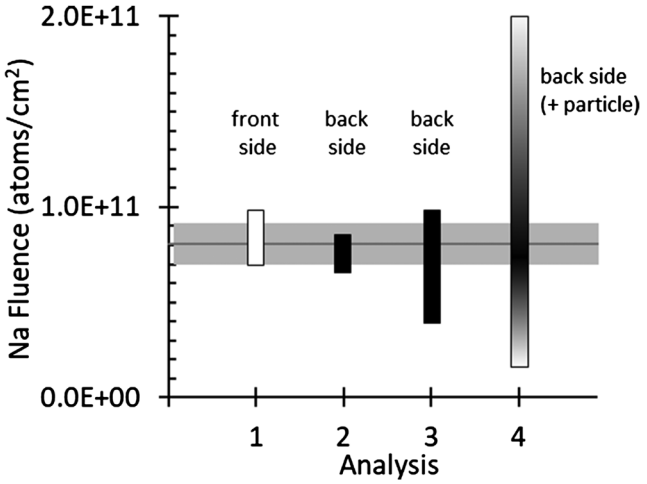

FIGURE 3 Comparison of Na results (DLC) from the front-side depth profile (white) with those of the back-side depth profiles (black, gradient). Each bar is the range of values resulting from a variety of SRIM fits. The gray horizontal box estimates the area of overlap between the front- and back-side results. It was calculated by (1) selecting SRIM fits for each analysis that the authors felt were based on the most reasonable assumptions, (2) averaging those select SRIM fits to find the average fluence for each analysis, and then (3) averaging the four averages (gray line) and taking the standard deviation of the averages. Gradient vertical bar indicates a clearly inhomogeneous DLC matrix.

The analysis labeled as "4" in Figure 3 was the largest source of uncertainty for calculating the width (fluence range) of the horizontal gray box, because there were several possible reasons for the apparent inhomogeneity of this sample of DLC. Moreover, various assumptions about the matrix properties in the SRIM fits could give wildly different answers, as shown by the size of the bar. Although the intensity data looked fine on a linear scale, the probable reason for the issue with inhomogeneity became obvious when the data were plotted on a log scale (Figure 4). Note that the backgrounds in the regions of the orange boxes in Figure 4 are not flat. Lower values in the range are likely the most realistic, as the higher values are likely due to a contaminant, e.g. a Na-containing particle. Integrating over what is likely a particle results in artificially high Na fluences. Accordingly, most of the fits we considered for analysis 4 avoided integrating this feature.

4 | DISCUSSION

Before this work, very few people published methods for precise, quantitative SIMS analysis in DLC and other than Rieck[1] we know of

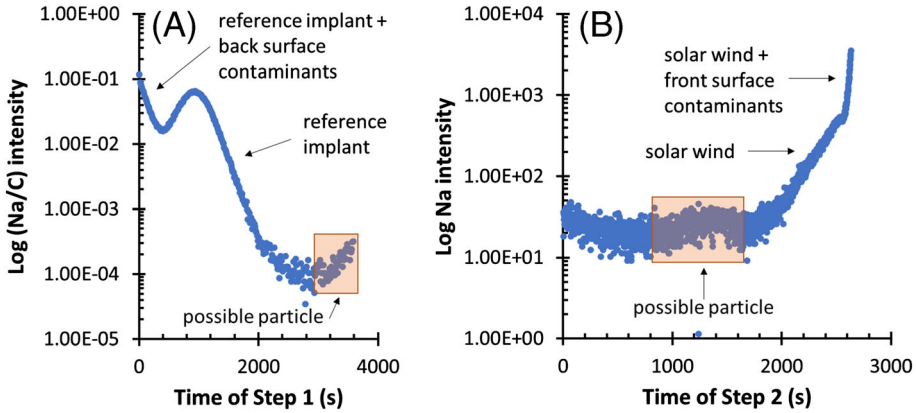

FIGURE 4 Uncorrected data from analysis 4 in Figure 3. (A) Matrix-normalized Na intensity for the implant. Notice that instead of going to background at the end of step 1, the concentration of Na appears to increase (tan box). (B) Na intensity (i.e. assumes constant C intensity). Notice that Na in the depth profile decreases at the beginning, suggesting that it was slowly going to background after the excursion in counts at the end of step 1. In addition, there is a second increase of Na counts at the start of the SW implant (tan box). Most likely, the tan boxes in both (A) and (B) are artifacts from embedded particulates, as the C count rate in (A) should have mitigated any small excursions in beam current. [Color figure can be viewed at wileyonlinelibrary.com]

no one who has tried calibration with reference ions implanted on the side of the DLC film where the silicon wafer had been removed. Because the electrical properties of DLC films are reported to be uniform with depth,[21] inhomogeneity with depth was not envisioned as a possible issue when this work was begun. However, we soon realized that, because the texture (the size and ratio of sp^3 and sp^2 domains) of the DLC films is known to vary somewhat with depth and that minor differences in Si concentration may affect ion yields,[8] we wondered if the Si concentration might increase in the zone of matrix near the DLC–silicon interface. So, it suddenly became important to look at the possibility that the matrix of the back-side implant was not matrix appropriate for analyses near the front surface. This unexpected facet of the study became imperative when Heber et al.[15] reported Na fluences from Genesis silicon that were unexpectedly large, outside the range of the errors in Figure 3 (see previous literature[1,15,23] for details on SW Na from silicon). However, the reproducibility of the front-side internal standard with the back-side internal standard in Figure 3 settles this issue. The higher fluence of SW Na from silicon is likely due to radiation-enhanced diffusion. A full discussion of this conclusion is beyond the scope of this work; however, a preliminary discussion is given in Rieck et al.[23]

There is, however, one possible effect of the changing texture with depth that we did notice. In all analyses, the change in the $^{12}C^+$ intensity did not correspond exactly with the inferred drift in the primary ion beam intensity. Specifically, in all cases, the $^{12}C^+$ intensity at depth seemed lower than what might be estimated from the beam current drift alone (e.g. Figure 5 – a sample matrix profile with nominally constant beam current). A test after the fact with an O_3^- beam (on the SIMS instrument with a Hyperion source that was available at the time) showed that, although the $^{12}C^+$ dropped slightly, the $^{12}C_2{}^+/^{12}C^+$ ratio was constant in the matrix through the back-side reference implant within our ability to measure it. Since $^{12}C_2{}^+$ and $^{12}C^+$ have different energy spectra, it is an indicator of local changes in electrical conductivity[8]: DLC with enough Si (or connected sp^2 bonds) to change the matrix properties would also increase the electrical conductivity.[8] Accordingly, the significant drop in $^{12}C^+$ through the zone of the internal standard during the back-side analyses may only be a SIMS artifact. We note that when the data were corrected using the drift of the beam current instead of normalizing to $^{12}C^+$, resultant fluences were more scattered. This result suggests that *if* the intensity of the $^{12}C^+$ reflects a matrix effect (i.e. an increased number of sp^2 bonds relative to sp^3, but not enough connected sp^2 domains to change the electrical conductivity) *then* the $^{23}Na^+$ intensity follows the concentration of increased $^{12}C^+$ from the sp^2 domains.

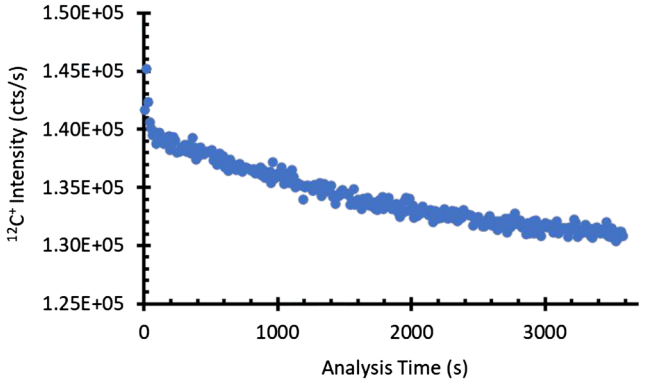

FIGURE 5 $^{12}C^+$ intensity versus time for back-side depth profile having a constant primary beam current. Fluences calculated over C-normalized data are internally consistent despite changing matrix counts at constant beam current.[8] This is a property of the matrix, not the SIMS analysis. [Color figure can be viewed at wileyonlinelibrary.com]

5 | SUMMARY AND CONCLUSIONS

Internal standardization is where a calibrated fluence of reference ions is implanted directly into the sample. Traditional front-side depth profiling of a shallowly implanted sample using a front-side-implanted internal standard can be complicated by transient sputtering, surface contamination, and interference with the unknown implant if the species is monoisotopic. BDP using internal standardization from the back side avoids these issues and allows measurement of both the standard and unknown in the same column without switching samples.

The primary benefits of internal standardization are that (1) it allows analyses to be performed without stopping to change between the sample and the standard, (2) the sample and standard are in the exact same position on the stage, and (3) any tilt or other mounting anomaly is present in both sample and standard, and the risk of changing the focus or of other analytical conditions changing between analysis of the standard and unknown is greatly reduced. Previous work used internal standardization by implanting reference ions from the front side, through the near-surface layer containing the unknown being measured. There are drawbacks to front-side internal standardization – especially for the analysis of monoisotopic ions – with the major issue being that the unknown and internal standard need to be deconvolved if there is overlap. Accordingly, this work investigated a new SIMS technique: BDP with back-side internal standardization.

Initially, the back-side reference internal standard was to be calibrated using this technique (i.e. implanting a reference implant in the back side of a second back-side-thinned, calibrated, well-characterized silicon standard). However, that sample was accidentally destroyed during preparation so external standards were used to calibrate our internal reference ion implant.

The back-side internal standardization with BDP was validated by comparing results from a sample having the same reference ions implanted into the front side of our sample (i.e. a front-side internal standard that passed through the "unknown" implant consisting of SW Na) with our purely back-side data. Although the front-side implant required some deconvolution from the SW in order to quantify the SW implant, the calculated SW fluence was the same within error in the front- and back-side-implanted samples.

From our perspective, our primary issues were in determining the depth of the crater and uneven sputtering through the collection surface due to small sample tilts or sample roughening. In our case – measurement of SW ions by SIMS analysis (positive secondary ions) –

the problem of locating the collection surface and of ion mixing near the epoxy–sample interface was resolved using the well-characterized SW ^{24}Mg ion as an *in situ* reference marker.[23]

Although our methods were demonstrated here using analyses of Na in DLC, our methods should be applicable to a broad range of other elements and matrices.

ACKNOWLEDGMENTS

This work has been supported in large part by National Aeronautics and Space Administration (NASA) Laboratory Analysis of Returned Samples grants. Specifically, support at ASU and Caltech was provided by 80NSSC22K0589 (A.J.G.J.) and NNX09AC35G (D. S. Burnett and A.J.G.J.). Support at LANL was provided by NASA awards NNH15AZ67I and NNH09ZDA001N (R.C.W. and K.D.R.). Support at NMC and LANL was provided by 80NSSC19K1239 (K.D.R. and R.C.W.). This work has also been supported by the NASA Earth and Space Science Fellowship: PLANET14R-0012 (NASA Earth and Space Science Fellowship 2012-13, 2013-14, and 2014-15; R.L.H. and K.D.R.; ASU).

SIMS analyses performed at the Arizona State University National SIMS Facility were supported by the National Science Foundation's (NSF) Division of Earth Sciences (EAR0622775). Use of the Center for Nanoscale Materials at Argonne National Laboratory was supported by the US Department of Energy, Office of Science, Office of Basic Energy Sciences (Contract DE-AC02-06CH11357).

Special thanks to the Genesis curation team at Johnson Space Center, the Secondary Ion and Mass Spectrometry Lab (ASU), the Center for Meteorite Studies (ASU), the W. M. Keck Foundation Laboratory for Environmental Biogeochemistry (ASU), the Caltech Microanalysis Center, the UCLA MegaSIMS Laboratory, the LeRoy Eyring Center for Solid State Science (ASU), the NanoSIMS Facility (ASU), the Secondary Ion and Mass Spectrometry Lab (WUSTL), Leonard Kroko Inc., D. S. Burnett, F. Stevie, V. Heber, I. V. Veryovkin, C. Miller, and C. Jones.

PEER REVIEW

The peer review history for this article is available at https://publons.com/publon/10.1002/rcm.9454.

DATA AVAILABILITY STATEMENT

The data that support the findings of this study are openly available in the Astromaterials Data Repository (AstroRepo) at https://doi.org/10.26022/IEDA/112732.[24]

ORCID

Karen D. Rieck https://orcid.org/0000-0002-7427-9134

REFERENCES

1. Rieck KD. Solar wind sodium and potassium abundance analysis in Genesis diamond-on-silicon and silicon bulk solar wind collectors, and how hydration affects the microtexture of olivine phase transformation at 18 GPa. Doctoral dissertation. Tempe, AZ: Arizona State University; 2015. https://hdl.handle.net/2286/R.I.36456
2. Jurewicz AJG, Burnett DS, Woolum DS, et al. Solar-wind Fe/Mg and a comparison with CI chondrites. *42nd Lunar Planet Sci Conf*., March 7–11, 2011; The Woodlands, TX. LPI Contribution No. 1608, Abstract #1917.
3. Burnett DS, Barraclough BL, Bennett R, et al. The Genesis discovery mission: Return of solar matter to earth. *Space Sci Rev*. 2003; 105(3–4):509-534. doi:10.1023/A:1024425810605
4. NASA Jet Propulsion Laboratory. GENESIS: Search for Origins. https://solarsystem.nasa.gov/genesismission/indexold.html. Accessed July 13, 2021.
5. Allton JH, Stansbery EK, McNamara KM. Size distribution of Genesis solar wind array collector fragments. *36th Lunar Planet Sci Conf*., March 14–18, 2005; League City, TX. LPI Contribution No. 1234, Abstract #2083.
6. Goreva YS, Allums KK, Gonzalez CP, et al. Genesis solar wind collector cleaning assessment: Update on 60336 Sample Case Study. *46th Lunar Planet Sci Conf*., March 16–20, 2015; The Woodlands, TX. LPI Contribution No. 1832, Abstract #2333.
7. Humayun M, Burnett DS, Jurewicz AJG. Preliminary magnesium isotopic composition of solar wind from Genesis SOS. *42nd Lunar Planet Sci Conf*., March 7–11, 2011; The Woodlands, TX. LPI Contribution No. 1608, Abstract #1211.
8. Jurewicz AJG, Olinger CT, Burnett DS, et al. Quantifying low fluence ion implants in diamond-like carbon film by secondary ion mass spectrometry by understanding matrix effects. *J Anal At Spectrom*. 2021;36(1):194-209. doi:10.1039/d0ja00375a
9. Janakiraman Paramasivan G, Sharma M, Jurewicz A, Burnett D. A procedure to cleanly separate solar wind osmium embedded in Genesis silicon collectors. *49th Lunar Planet Sci Conf*., March 19–23, 2018; The Woodlands, TX. LPI Contribution No. 2083, Abstract #2886.
10. Huss GR, Koeman-Shields E, Jurewicz AJG, et al. Hydrogen fluence in Genesis collectors: Implications for acceleration of solar wind and for solar metallicity. *Meteorit Planet Sci*. 2020;55(2):326-351. doi:10.1111/maps.13420
11. Bajo K-I, Olinger CT, Jurewicz AJG, et al. Depth profiling analysis of solar wind helium collected in diamond-like carbon film from *Genesis*. *Geochem J*. 2015;49(5):559-566. doi:10.2343/geochemj.2.0385
12. Jurewicz AJG, Rieck KD, Hervig R, et al. Magnesium isotopes of the bulk solar wind from Genesis diamond-like carbon films. *Meteorit Planet Sci*. 2020;55(2):352-375. doi:10.1111/maps.13439
13. Burnett DS, Jurewicz AJG, Woolum DS, et al. Ion implants as matrix-appropriate standards for geochemical ion probe analyses. *Geostand Geoanal Res*. 2015;39(3):265-276. doi:10.1111/j.1751-908X.2014.00318.x
14. Heber VS, McKeegan KD, Burnett DS, et al. Accurate analysis of shallowly implanted solar wind ions by SIMS backside depth profiling. *Chem Geol*. 2014;390:61-73. doi:10.1016/j.chemgeo.2014.10.003
15. Veryovkin IV, Zinovev AV, Tripa CE, Burnett DS. Depth profiling of Genesis diamond-on-silicon collectors: Direct comparison between frontside and backside approaches. *45th Lunar Planet Sci Conf*., March 17–21, 2014; The Woodlands, TX. LPI Contribution No. 1777, Abstract #2795.
16. Paque JM, Hofmann AE, Burnett DS, et al. Electron microprobe/SIMS determinations of Al in olivine: Applications to solar wind, pallasites and trace element measurements. *Geostand Geoanal Res*. 2020;44(3): 473-484. doi:10.1111/ggr.12347
17. Waeselmann N, Humayun M, Goreva YS, Burnett DS, Jurewicz A. Impact of acid-cleaning on the solar wind layer of Genesis flight wafers – Partial dissolution and recovery of the lithium-6 implant. *46th Lunar Planet Sci Conf*., March 16–20, 2015; The Woodlands, TX. LPI Contribution No. 1832, Abstract #1266.
18. Westphal AJ, Ogliore RC, Huss GR, Nakashima K, Olinger C. Mg profile correction in Genesis Si collectors using rastered ion imaging.

45th Lunar Planet Sci Conf., March 17–21, 2014; The Woodlands, TX. LPI Contribution No. 1777, Abstract #2671.
19. Sinha D. Correlating chemical and water purity to the surface metal on silicon wafer during wet cleaning process. *Chem Eng Commun*. 2002;189(7):974-984. doi:10.1080/00986440213129
20. Sullivan JP, Friedmann TA, Dunn RG, et al. The electronic transport mechanism in amorphous tetrahedrally-coordinated carbon films. *Mater Res Soc Symp Proc*. 1998;498(1):97-102. doi:10.1557/PROC-498-97
21. Wilson RG, Stevie FA, Magee CW. *Secondary Ion Mass Spectrometry: A Practical Handbook for Depth Profiling and Bulk Impurity Analysis*. New York, NY: John Wiley and Sons, Inc.; 1989.
22. Rieck KD, Jurewicz AJG, Ogliore RC. Comparing SIMS data for solar wind Na in two collectors using multiple approaches. *52nd Lunar Planet Sci Conf*., March 15–19, 2021; The Woodlands, TX. LPI Contribution No. 2548, Abstract #2638.
23. Heber VS, McKeegan KD, Steele RCJ, et al. Elemental abundances of major elements in the solar wind as measured in Genesis targets and implications on solar wind fractionation. *Astrophys J*. 2021;907(1):15. doi:10.3847/1538-4357/abc94a
24. Rieck KD, Jurewicz, AJG, Hervig RL, Williams P, Olinger CT, Wiens RC, Ogliore RC. Raw SIMS depth profiling data from internally standardized diamond-like carbon Genesis solar wind collectors., Version 1.0. Interdisciplinary Earth Data Alliance (IEDA). 2024. https://doi.org/10.26022/IEDA/112732. Accessed 2023-01-05.

SUPPORTING INFORMATION

Additional supporting information can be found online in the Supporting Information section at the end of this article.

How to cite this article: Rieck KD, Jurewicz AJG, Hervig RL, et al. Depth profiling and standardization from the back side of a sample for accurate analyses: Emphasis on quantifying low-fluence, shallow implants in diamond-like carbon. *Rapid Commun Mass Spectrom*. 2023;37(6):e9454. doi:10.1002/rcm.9454